中国工程机械学会
CHINESE CONSTRUCTION MACHINERY SOCIETY
ccms

ICACMVE'11

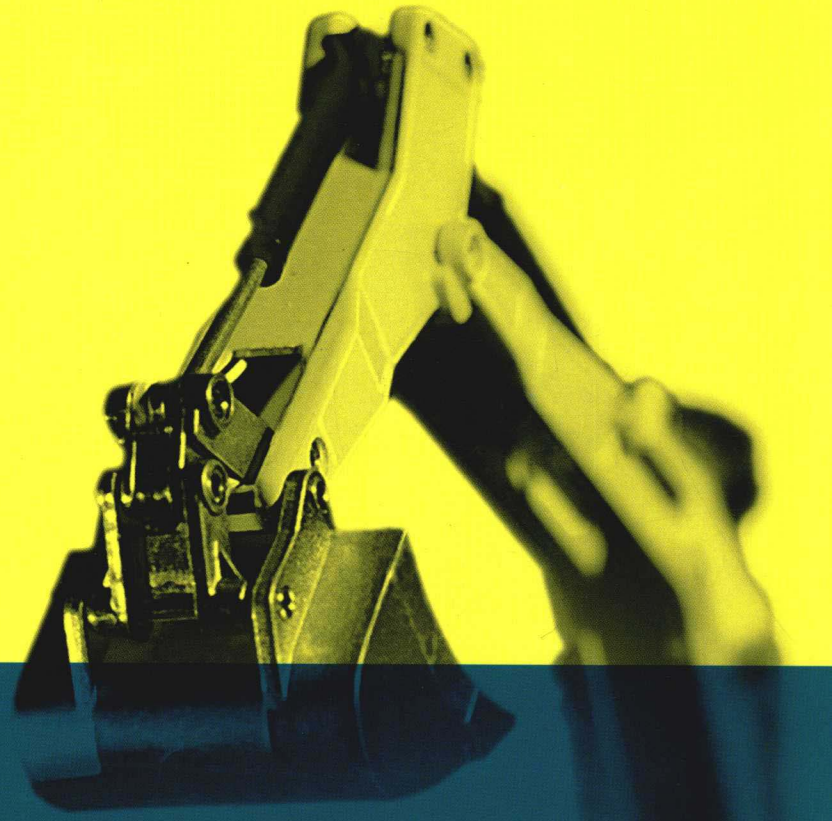

Editor-in-chief Shi Laide

Proceedings of the 2011 International Conference on Advances in Construction Machinery and Vehicle Engineering

中国工程机械学会 编
Chinese Construction Machinery Society

上海科学技术出版社
Shanghai Scientific & Technical Publishers

Proceedings of the 2011 International Conference on Advances in Construction Machinery and Vehicle Engineering

中国工程机械学会　编

Chinese Construction Machinery Society

editor-in-chief　Shi Laide

ICACMVE' 2011

Sponsored by Chinese Construction Machinery Society (CCMS)

Organized by Tongji University, China Shanghai Maritime University

Jointly Sponsored by National Natural Science Foundation of China, China Administration Committee of Changsha National Economic and Technical Development Zone, China

上海科学技术出版社

Shanghai Scientific & Technical Publishers

图书在版编目(CIP)数据

2011 工程机械与车辆工程新进展国际学术会议论文集=Proceedings of the 2011 International Conference on Advances in Construction Machinery and Vehicle Engineering：英文/中国工程机械学会编. 上海：上海科学科技术出版社， 2011.3
ISBN 978-7-5478-1195-5

Ⅰ.①2… Ⅱ.①中… Ⅲ.①工程机械—国际学术会议—文集—英文 ②车辆工程—国际学术会议—文集—英文
Ⅳ.①TU6-53②U27-53

中国版本图书馆 CIP 数据核字（2012）第 017696 号

Brief Introduction

The 2011 International Conference on Advances in Construction Machinery and Vehicle Engineering (ICACMVE'2011) is one of the academic conferences originated by Chinese Construction Machinery Society(CCMS), and it was organized by Tongji University and Shanghai Maritime University, and jointly sponsored by National Natural Science Foundation of China and Administration Committee of Changsha National Economic and Technical Development Zone of China. After peer-reviewed, 140 papers presented by participants from China, United States of American, Germany, Japan, Russia, Canada, Australia, the Netherlands and Singapore were accepted for publication. The proceedings offered an opportunity of bring together worldwide academic researchers and industrial practitioners for the interchange of information on the latest development and applications in Construction Machinery and Vehicle Engineering technology. It is our sincere hope that researchers and developers will benefit from these papers.

上海世纪出版股份有限公司
上 海 科 学 技 术 出 版 社 出版、发行
（上海钦州南路 71 号 邮政编码 200235）

新华书店上海发行所经销
苏州望电印刷有限公司印刷
开本 889×1194 1/16 印张：39.75
字数：760 千字
2012 年 3 月第 1 版 2012 年 3 月第 1 次印刷
ISBN 978-7-5478-1195-5/TU・149
定价：180 元

Contents

Introduction to Keynote Speeches on ICACMVE'2011

1 New Design & Development of Product Design Methodology

By Prof. Dr. Bangchun WEN, Northeastern University, China
Abstract This keynote speech firstly introduced the classification of 70 design methods. And we can understand the general and special design cases much easier after the classification. Then four novel design methods were studied in details, including investigation, planning, synthetic design and quality assessment, which made great improvements in the innovation design. Finally, the product harmonious design and deep-layer design were discussed in the speech. And there should be a harmonious balance among products and nature environment, society environment technology market and fund environment, and policy environment.

2 Sensor System and Cable Robotics for Vehicles

By Prof. Saman HALGAMUGE, Department of Mechanical Engineering, Melbourne School of Engineering, Australia
Abstract In the beginning of the keynote speech, the speaker started with a quick glance at the mechatronics, which was a mixture of technologies and techniques that together help in design better products. Then the speech gave a detailed introduction of the driver support system about how to help the car save more fuel. In order to monitor the large spaces, a strategy to maximize the performance of the network by managing the orphaned nodes was also proposed. The keynote speech was ended with the introduction of cable robots and an optimization case of cable driven system.

3 Transform and Cooperate

By Prof. Dr. Chongqing GUO, Tongji University, China
Abstract In this keynote speech, the speaker firstly revealed the future development way in the nowadays society. The development of the cloud strategy and sea strategy would become the pattern of innovation for all industries. Then the speaker introduced the conception of Services Sciences, Management, and Engineering (SSME) and the necessity of the service innovation, especially the present situation of China's industrialization. Finally, the speaker emphasized the changes induced by the times development. Due to the imagination and creativity of the new generation students, the future education function should consider the liberation of the human language, communication, observation, reasoning, imagination and creative potential.

4 Dynamic Maintenance towards a New Maintenance Approach

By Prof. Dr. Ir. J.Ph.C. Wubben Msc, Zeeland University, Netherlands
Abstract In order to minimize costs, as well as sustain the desired availability and safety, the speaker firstly indicated that the new maintenance development is necessary. The speaker not only stated the impact and the importance of the maintenance method for the mechanical industry, but also analyzed the problems to be solved in this field. Then the speaker presented the dynamic maintenance's advantages by taking a concrete example. Finally, the differences between the static and the dynamic maintenance, as well as the maintenance strategy and method, all are completely introduced in the keynote speech.

5 The Path of Electric Vehicles Development of China

By Prof. Dr. Zhuoping YU, Dean of School of Automotive Studies, Tongji University
and Prof. Dr. Zechang SUN, School of Automotive Studies, Tongji University
Abstract Chinese automobile industry has experienced a rapid development in the past decades, which makes China the largest producer of automobiles of the world. This keynote speech begins with the challenges caused by the rapid development of electric vehicles, such as energy saving and emission problems. After that, the development plan of China for electric automobiles was introduced in details. Finally, the electric vehicle development and achievement of China were summarized and discussed in different aspects, including Hybrid Electric Vehicles (HEV), Battery Electric Vehicles (BEV), key components and parts (e.g. Power Cell, E-motor, Fuel Cell), integration and control techniques of power system, hydrogen energy for automobiles. The role and relevant achievement of the Tongji University in the development of electric vehicles were also presented.

6 Sustainable Product Conceptualization for Green Automobiles

By Prof. Dr. Chun-Hsien CHEN, Associate Editor, Advanced Engineering Informatics, Director of Design Stream; School of Mechanical Aerospace Engineering, Nanyang Technological University, Singapore
Abstract In the beginning of the keynote speech, the background, objective and architecture of Sustainable Product Conceptualization (SPC) were introduced. The key technologies of SPC were discussed subsequently, including laddering, Design Knowledge Hierarchy (DKH) and Hopfield Network. The design of a cellular phone was presented as a case study for SPC to illustrate the application of the key technologies. The speech was ended with the discussions on the development of green cars, e.g. electric and fuel cell powered, partly fuel and partly electric or fuel cell powered, alternative fuels powered, compressed air powered and solar energy powered cars, and the achievement of Nanyang Technological University in this area, such as solar energy powered cars and diesel fuel powered cars.

7 New HST Makes Easy Utilization of Ocean Wave Energy

By Prof. Dr. Tomiji WATABE, T-Wave Consultant, JAPAN

Abstract Ocean wave has a rich energy density and therefore its utilization is inherently reasonable, if the conversion of wave energy could be improved to the same degree as what has been done for wind energy conversion. In this keynote speech, the nature of the ocean wave energy firstly was introduced. And then Ocean Wave Energy Systems (OWES), which belong to the Moving Body Type (MBT) and apply the HST in its conversion principle, were proposed and recommended as an efficient energy conversion device and are expected to supply the practical electricity instead of the burning type power plants in the near future. HST is the key technology of OWES and has to be improved to cover such the high power level for the future needs. The system principle, the typical structure and the HST for the future MBT were investigated and discussed subsequently to show the new technologies on the OWE utilization.

8 Advancing the Industry through Clean and High Efficiency Technologies – What Can We Learn from US Super Truck Program

By Dr. Ning LEI, Technical Fellow, Powertrain Engineering of Navistar Inc.

Abstract In this keynote speech, the speaker began with a quick glance at the main business segments and a brief summary of the history of Navistar. Navistar today was then presented in two aspects, i.e. its market strategy (North America focus, global growth) and its new product series (wide range engine products, IC bus global product portfolio, in-house specialty vehicles and specialty vehicles with its alliances/technical partners). After that, the background and highlights of US DoE Super Truck Program, as well as Navistar's measurements and achievement in this program were discussed. Finally, the knowledge from US Super truck program and Navistar's relevant experiences were shared, i.e. invest in future key clean efficiency technology, increase the government/industry/university collaboration, fuel quality is key and need to be improved, leverage the knowledge from US and others.

9 High Efficiency Clean Combustion Engines Trends in Control and Hardware Improvements

By Prof. Dr. Ming ZHENG, University of Windsor, Canada

Abstract Nowadays, energy crisis and air pollution are very urgent all around the world. Due to its low emission and high efficiency, low temperature combustion mode has drawn more and more attention and could be run with different kinds of fuel. To meet the more stringent emission limitation or even zero emission, in-cylinder low temperature combustion with smart control, HP&LP EGR, VVT, boost, multi injection and active exhaust gas after-treatment should be utilized. And fuel efficiency designs must comply with the ultimate emission goals and be capable of using bio-fuels. The fuel preference for Low Temperature Combustion and the control strategy were summarized and propose in details at the end of the keynote speech.

10 Mixture Formation Process of a Flexible Valve Train DI Gasoline Engine with Side-Mounted Multi-Hole Injectors

By Prof. Ming-Chia LAI, Wayne State University, USA

Abstract Advanced valvetrain coupled with Direct Injection (DI) provides an opportunity to simultaneous reduction of fuel consumption and emissions. Because of their robustness and cost performance, multi-hole injectors are being adopted as gasoline DI fuel injectors. Ethanol and ethanol-gasoline blends synergistically improve the performance of a turbo-charged DI gasoline engine, especially in down-sized, down-sped and variable-valvetrain engine architecture. The keynote speech presents Mie-scattering spray imaging results taken with an Optical Accessible Engine (OAE). OAE offers dynamic and realistic in-cylinder charge motion with direct imaging capability, and the interaction with the ethanol spray with the intake air is studied. Two types of cams which are designed for Early Intake Valve Close (EIVC) and Later Intake Valve Close (LIVC) are tested, and the effect of variable valve profile and deactivation of one of the intake valves are discussed. Multi-dimensional Computation Fluid Dynamics (CFD) results for predicting DI multi-hole ethanol spray behaviors are presented as well. The effects of injection timing on the bulk flow motion and fuel-air mixing, in terms of tumble and swirl ratios, turbulence, and fuel wall film behaviors are discussed. Combined with metal engine test results which run with gasoline, the important mechanisms for reducing fuel consumption and emissions in a SIDI, variable-valve actuated engine are demonstrated.

11 X-ray Microimaging of Engine Sprays of Conventional and Alternative Fuels

By Dr. Jin WANG, Argonne National Laboratory, Argonne, IL 60439, USA

Abstract Sprays of conventional and alternative fuels are part of energy sources for propulsion and transportation systems including internal combustion engines, where fuel breakup and atomization is the first and crucial step for combustion. During a high-pressure liquid injection process, the highly transient nozzle geometry ultimately determines the boundary conditions for the in-nozzle flow, and hence, the jets or sprays exiting the orifice. In this keynote speech, ultrafast x-ray propagation-based microimaging technique was used to obtain high-spatial-resolution and single-shot images of the dense diesel and biodiesel fuel jets in the near-nozzle region issuing into a quiescent nitrogen gas ambient. The results show that the jet morphology is highly sensitive to jet velocity, nozzle geometry and the physical properties of fuels. The first in situ ultrafast synchrotron X-ray microimaging is used to visualize the transient internal dynamics in injection nozzles during a millisecond injection process, where the valve dynamics have the most direct effects on the spray formation immediately outside of the nozzle. The transient measurement enabled a transient numerical simulation of the liquid flow inside the nozzle.

Numerical Simulation Research on Hydraulic Stewart Force Feedback Manipulator

Hou* Jingwei, Zhao Dingxuan, Shang Tao

College of Mechanics Science and Engineering Jilin University, Changchun 130025, China
* Corresponding Author: houjw@jlu.edu.cn

Abstract A novel force feedback joystick which has a hydraulic actuated Stewart manipulator is developed. To provide an experiment platform for the control strategy design, a simulation program based on the simulator's control framework is developed with MATLAB/SimMechanic. In the program, the expected trajectory is generated by inverse kinematic, and servo valve and cylinder modules are actuated by a position control algorithm with P/D controller. The trajectory is generated according to the force on the platform. The force on the upper platform is calculated by the leg force, which can be used to realize force feedback function. It is proved by experiment that the program can realize the experiment function for control strategy design; its validity is verified by comparison between the result calculated manually and the result from the program during the static state.

Keywords Numerical simulation; Hydraulic servo-system; Stewart platform; Comparison experiment.

1 Introduction

If the kinematic chain of a mechanism can form at least one closed loop, it is called parallel mechanism, otherwise known as the serial mechanism[1]. Typically, to increase the robot's degrees of freedom, a serial mechanism will have to add the new joints, which results in accumulation of errors. The parallel mechanism not only produces cumulative errors, but also provides multiple degrees of freedom in a smaller space. This feature makes it the hot spot in the current multi-DOF joystick and robot joint design.

Jun Murayama[2] etc. presented a 6 DOF virtual haptic device constructed by a pair of string-based parallel manipulator named as SPIDAR G&G. Zhang[3] presented a Exoskeleton Based Man Marching Intelligent System by a 3 DOF parallel mechanism.

In 2000, Kudomi, Muto et al[4] established a hydraulic driven Stewart-type master-slave force feedback system. Both the master hand and the slave hand of the system are Stewart mechanisms. In the system, the operator operates a grinding robot by master-slave control to avoid the operator to work in the full location harmful dust. Professor Zhao Dingxuan[5] in Jilin University has improved it from the design, then a new control framework driven from the slave side is put forward, thereby enhancing its dynamics. Here in this paper we developed a MATLAB/Simmechanics program to simulate the master hand of the master-slave, which can be used in simulation experiment.

In this paper, we introduced the structure of the master -slave system in Section 2, and then the simulation program was introduced in Section 3; we did an experiment to test its function and validity in Section 4.

2 The component of the motion simulator

The master hand of the master-slave system is shown in Fig.1. Its upper platform and the lower platform are connected by six cylinders; the cylinders can stretch out and draw back independently. They are linked by universal joints partly, the upper platform can move simultaneously in all six degrees. The displacements of the hydraulic cylinders can be detected by position sensors equipped on the tube. The force at the master hand is acquired by 6-DOF sensor.

The system works as following: the master driving force of the hand sensor is derived by dynamics calculation to present the leg forces. The force is then multiplied by a coefficient and subtracted by the slave force; the error can be used as the control signal to control the master hand to move. The master movement passed to the slave hand and it will follow the master movement.

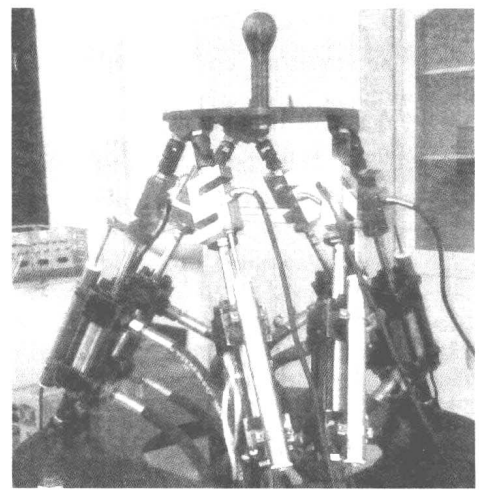

Fig.1 The hydraulic Stewart manipulator

3 The simulation program

3.1 The component of the simulation program

Based on the system described in Section 2, we developed a simulation program by MATLAB/SimMechanics, as shown in

Fig.2. The system consists of four parts - trajectory generator; controller; motion platform and force calculator.

The mechanical components of the Stewart Platform consist of a top plate, a bottom plate, and six legs connecting the top plate to the bottom plate. The overall system has six degrees of freedom. Each leg subsystem contains two bodies connected together with a cylindrical joint. The upper body connects to the top mobile plate using a universal joint, and the lower body connects to the base plate using a second universal joint.

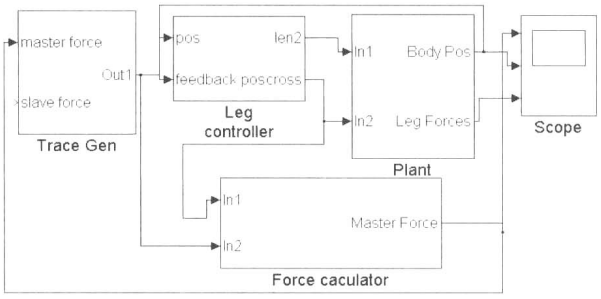

Fig. 2 The simulation program

The basic goal of the trajectory generator is to specify the desired trajectory of the upper plate in both position and orientation according to the force error and dynamic parameters. We then map this desired trajectory to the corresponding trajectory in the legs using inverse kinematics. Finally, we use a lower level controller for each leg to command the leg to follow the desired trajectory. The leg trajectory generates the desired leg lengths for each time step. It starts with a desired rotation and position of the top plate and calculates the desired leg lengths to achieve this.

The controller is designed based on the classic PID design and the mathematics model of the hydraulic system. The input to this controller is the actual leg position and velocity and the desired leg position. By the mathematics model of the hydraulic system that will be introduced in Section 3.2, the force that to be input to the plant model is generated[6, 7].

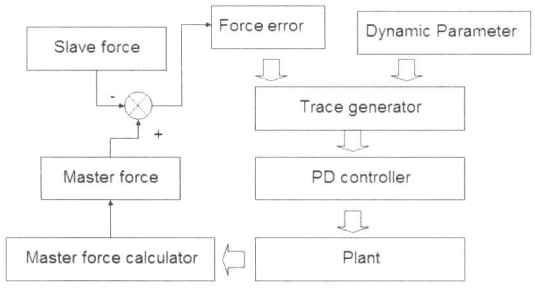

Fig. 3 The work process of the program

3.2 Mathematics model of the hydraulic system

The equation of motion of the servo valve is given by Eq. (1).

$$\frac{d^2x}{dt^2} + 2\zeta\omega_n \frac{dx}{dt} + \omega_n^2 x = k_v \omega_n^2 i \tag{1}$$

The equation of motion of the piston is given by Eq. (2).

$$\left.\begin{aligned} m\ddot{y}_s + b\dot{y}_s &= a_p p_L \\ p_L &= p_a - p_b \end{aligned}\right\} \tag{2}$$

The relations for flow rate q_L are given by Eqs. (3) and (4).

$$q_t = k_x x - k_p p_t \tag{3}$$

$$q_t = a_p \dot{y}_s \tag{4}$$

The parameters are as the following:

a_p	: Cross-sectional area of piston	[m^2]
a_{pa}, a_{pb}	: Area of piston	[m^2]
b	: Viscous damping coefficient of piston	[Ns/m]
k_a	: Gain of servo amplifier	[mA/V]
k_x, k_p	: Flow rate gain, pressure gain	[m^2/s], [m^4/kg]
k_v	: Gain of servo valve	[m/mA]
m_u	: Mass of upper platform	[kg]
m_p	: Mass of piston	[kg]
m_c	: Mass of cylinder	[kg]
p_a, p_b	: Pressures in piston chambers	[Pa]
q_L, p_L	: Flow rate, load pressure	[m^3/s],[Pa]
T	: Gain	[-]
u	: Control input	[V]
x	: Displacement of spool	[m]
ζ	: Damping ratio	[-]
ω_n	: Natural angular frequency	[rad/s]

Consequently the mathematical model of the slave system is represented by Eq. (1) to Eq. (4). With a Laplace transform, the equations can be expressed as Transfer Fun components in the Simulink library. The hydraulic subsystem is shown in Fig.4.

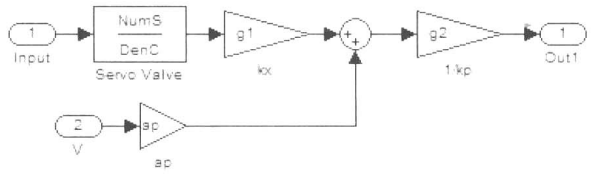

Fig. 4 The hydraulic subsystem

3.3 The force reflecting matrix

$$G = \begin{bmatrix} g_{21} & g_{22} & g_{23} & g_{24} & g_{25} & g_{26} \\ g_{31} & g_{32} & g_{33} & g_{34} & g_{35} & g_{36} \\ g_{41} & g_{42} & g_{43} & g_{44} & g_{45} & g_{46} \\ g_{51} & g_{52} & g_{53} & g_{54} & g_{55} & g_{56} \\ g_{61} & g_{62} & g_{63} & g_{64} & g_{65} & g_{66} \end{bmatrix} \bullet (1/L) \tag{5}$$

The function of the force reflecting matrix is to transform the leg force to the force act on the upper platform. In this paper, we use the Stewart static forward matrix as the force reflecting matrix. In Eq. (5), $\boldsymbol{G}$ is a 6×6 matrix; its parameters are described in Ref. [8].

4 Simulation experiment

To test the accuracy of the program, we did an experiment to compare between the force results of every cylinder by calculating manually and those from the program when the

upper plate is at three different positions and orientations. The parameters used in the program are shown in Table 1. To tell the result, we chose three points. The experiment's result is shown in Table 2.

Table 1 The parameters in the simulation program

k_u=1.0mA/V	k_v=0.144×10^{-3}mA/V
ω_n=354rad/s	ζ=0.1
w=4.8×10^{-3}m	m_c=0.801kg
δ=1.5×10^{-5}m	m_u=1.732kg
k_p=5.09×10^{-3}m^{4}s/kg	m_p=1.243kg
k_v=3.03×10^{-6}m^2/s	a_{pa}=1.26×10^{-5}m^2
b=44.3Ns/m	a_{pb}=0.76×10^{-5}m^2

Table 2 The force validate experiment result

The upper plate position and orientation $[x_p\ y_p\ z_p\ x_a\ y_a\ z_a]$	Force on every cylinder from simulation program $[f_1\ f_2\ f_3\ f_4\ f_5\ f_6]$	Force on every cylinder by calculating $[f'_1\ f'_2\ f'_3\ f'_4\ f'_5\ f'_6]$
[0 0 1 0 0 0]	[1.0294 1.0294 1.0294 1.0294 1.0294 1.0294] ×10	[1.0294 1.0294 1.0294 1.0294 1.0294 1.0294] ×10
[0.5 0.5 1 0 0 0]	[0.8212 1.7098 2.7613 -1.0239 -1.5381 1.5397] ×10	[0.8212 1.7098 2.7613 -1.0239 -1.5381 1.5397] ×10
[0.5 0.5 1 0.25 0.25 0.15]	[-0.0618 -4.4281 -4.9890 0.8158 1.7417 -0.6977] ×10	[-0.0618 -4.4281 -4.9890 0.8158 1.7417 -0.7010] ×10

From the result, we can know that the result from simulation program is very near to the one by calculating, so we can know that the program is right.

Another experiment to test the calculation of the force act on the upper platform was also done. In the experiment, we set the slave force as zero, and we force the upper platform to move on a circle in the XY plane and the mass of the legs are set to zero. Then ignore the effect of the friction, the force of the upper platform can be looked on as the resultant force of the centrifugal force. The following is the results of calculating manually and those from the program by the force of inverse dynamic. In the table 3, Angle is the angle in the absolute coordinate of the line between the position of the center point of the upper platform and the origin point. F_x, F_y are the force on the upper platform in the program, F_{xc}, F_{yc} are the force on the upper platform by manual calculation.

Table 3 The force calculation experiment result

Angle	F_x	F_{xc}	F_y	F_{yc}
0	6.928	6.901	0	0
π/3	-3.46	-3.460	5.982	5.988
2π/3	-3.46	-3.461	-5.982	-5.982

From the result, we can see that there is a small error between the calculating result and the program result because of the numerical calculation. But we can know that the result from simulation program is very near to the one by calculating, so we can know that the program is built right. We can also show the results during the simulating process by the scope control component. The result of the force calculation is shown in Fig.5.

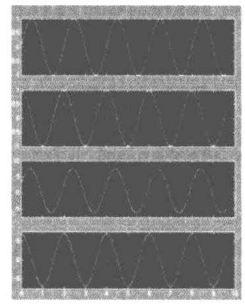

Fig. 5 Force calculation experiment result in scope

5 Conclusions

A simulation program for hydraulic Stewart platform is developed for control strategy design. In this paper, we did experiments to test the validity of the simulation results and the performance on calculating the work state of the motion simulator during work process. The result is good and program can be used widely for the research work on hydraulic Stewart platform.

Acknowledgments

Thanks to the Science and Technology Development Program Emphasis Project of Jilin Province (No. 20080506, No. 20090335).

References

[1] Vincent Hayward, Karon E. Maclean. Do It Yourself Haptics: Part I[J], IEEE Robotics & Automation Magazine, 2007.

[2] Jun Murayama, Laroussi Bougrila, YanLin Luo et al. SPIDAR G&G: A Two-Handed Haptic Interface for Bimanual VR Interaction[C], Eurohaptics 2004 Conference, June 5th-7th, Munich, Germany. 2004:1-9.

[3] Zhang Jiafan. Exoskeleton Based Man Maching Intelligent System and Its Application[D], Dissertation for the Doctoral Degree, Zhe Jiang University, 2009.

[4] S. Kudomi, H. Yamada, T. Muto. Development of a hydraulic parallel link type of force display[C], Proc. 5th JHPS Inter. Symp. on Fluid Power, 2002:471-476.

[5] Chen Tiehua, Zhao Dingxuan, Zhang Zhuxin. Design of Master-slave Manipulators System and Bilateral Servo Control Strategy[J]. Transactions of the Chinese Society for Agricultural Machinery, 2008, (12):141-145.

[6] C. Szep, S. Stan, V. Csibi, et al. Study of design, kinematics and accuracy modelling of 3 degrees of freedom robot[J], Mechanism and Machine Theory, 2008:77(3), 58-61.

[7] Chifu Yang, Qitao Huang, Hongzhou Jiang, et al. PD control with gravity compensation for hydraulic 6-DOF parallel manipulator[J], Mechanism and Machine Theory, 2010:45, 666-677.

[8] Zhao Yanzhi. Basic Theoretics And System Development On Wide Range Parallel Six-Component Force Sensor With Flexible Joints[D]. Dissertation for the Doctoral Degree, Yanshan University, 2008.

Motion Simulation Based on Virtual Reality

Zhao Dingxuan, Liu Songyue *, Ni Tao, Zhang Hongyan

College of Mechanical Science and Engineering, Jilin University, Changchun 130022, China
* Corresponding Author: liusongyuexin@126.com

Abstract Motion simulators are booming in recent years for vehicle system development, human factor study, and training of driving skills. In this paper, a new type of motion simulator is introduced with a hexapod steward motion platform as the base and a cab above with four Liquid Crystal Displays (LCDs) placed at the corresponding position. With the technique of synchronous record and synchronous representation, a six degree of freedom (6-DOF) motion will be rendered by the platform. In such a system, the one sitting in the cab can face the computer generated graphic images on the LCDs just as if looking through the real window in a vehicle. Besides, to enhance the visual effect of the simulation, stereo equipments are located in the corner of the cab. In the system, the immersion sense of the Virtual Reality can be achieved by the methods of movement, 3D images and sound effects.

Keywords Virtual Reality; Motion simulator; 6-DOF simulato; Kinematics; Synchronal record.

1 Introduction

Virtual reality (VR) is a cross-discipline, which consists of computer graphics (CG), image processing and recognition, computer simulation technology, man-machine interface technology, etc.

As the advantage of high efficiency, safety and low cost, the application of virtual reality attracts increasing attention. In this paper, virtual reality is used in the development of a motion simulation system, which is well accepted in driving training and other fields. Motion simulators are indispensable to the test for such critical situations as in a collision, a crash and a sliding[1-5].

However, despite the development of motion simulator, the DOF of the movement and the immersion sense of VR are limited. Although a great deal of research effort has been devoted to reducing the limitation, the existing research mainly pays attention to the kinematic mechanism and neglects the overall realism of motion simulation.

2 Structure of the motion simulation system

Similar to most of the advanced motion simulators around the world, our system has the same following common ground: first of all, a platform is used to provide the motion; secondly, more than three image generators are used for high-resolution graphic projection; and finally, high performance parallel-processed computers or a group of server computers are involved in the system for real-time graphics, 3D sounds and dynamics.

2.1 Physical configuration

The physical configuration of our motion simulation system consists of a hexapod steward motion platform and a cab mounted on, shown as the Fig. 1. The windows of the cab are replaced by four LCDs, as the approximately same size at the corresponding positions. Visual image generated by the graphic computer is divided into four channels and displays respectively on the front left, front right, side left, side right LCD windows of the cab. The multiple surrounding displays could provide a 180 degree forward field-of-view with incredible high immersion.

Besides, since sound rendering takes an important role in the immersion feeling of a motion simulation system, directional audio cueing is provided by multiple speakers in the corner of the cab. Spatial sound generation associating with wind, passing objects, and other environmental sources transmitted to the cab can significantly enhance the overall realism of a motion simulator.

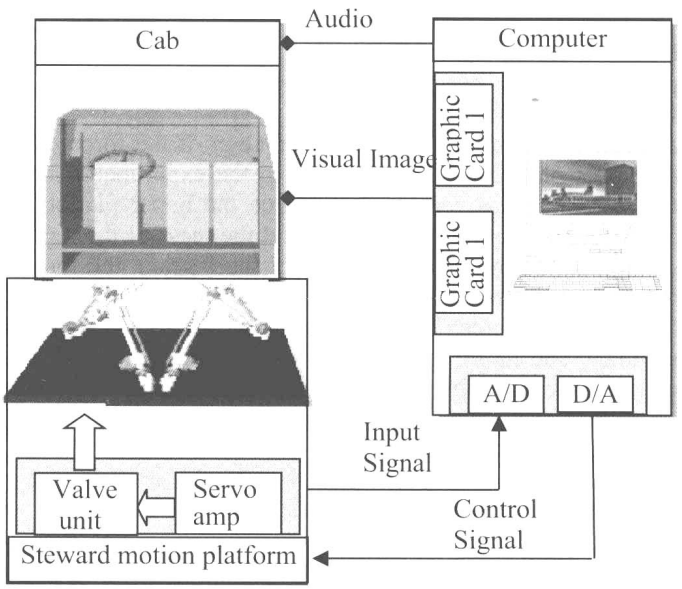

Fig. 1 System physical configuration

Thus, in our system, anyone sitting in the cab will be surrounded by stereoscopic 3D images rendered by four individual displays around. The input signals are sensed and transmitted to the computer by the method of synchronous record. Then, with the technique of synchronous representation, the simulation can be performed in real-time to present the motion and realistic graphic images as well as

the sound of the environment corresponding to conditions are recorded.

2.2 Software Architecture

Originally, we planned to select a commercial Virtual Reality engine named OpenGVS. However, OpenGVS has a node lock license and a high-cost, which limit the popularization of our motion simulator. Thus, the software of our simulation program is totally based on an open source game engine Delta3D. The overall architecture of the motion simulation software is described in Fig. 2

The Core of Delta3D is the Game Manager (GM), and it owns all the Actors, Components and Messages. All the active objects such as autonomous vehicles, moving person, dynamic terrain and the inactive objects including static terrain, light, sounds, etc., are included into the simulation software as Actors.

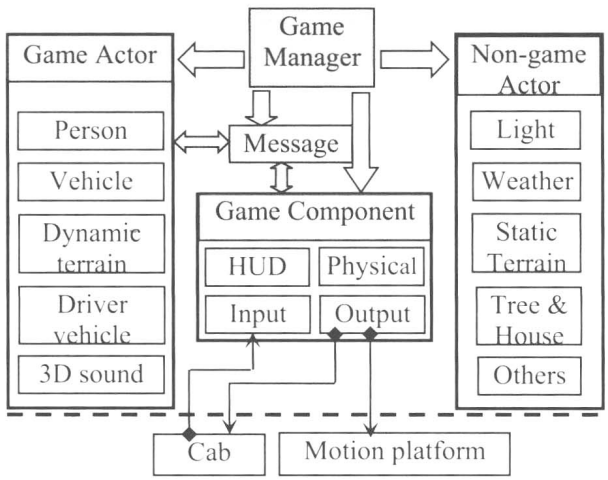

Fig. 2 System software architecture

Components are responsible for processing the Messages from the GM and deciding how to deal with the Messages. Here, Messages are user defined data used for the communication between Actors and Components. The HUD Component provides the graphic user interface (GUI), and the Physical Component is responsible for collision detection among all the Actors in the virtual world. The Input Component just gets the manipulation signals through computer's serial port and sends these signals to the Dynamic Module (DM) of motion simulator Actor. It is the DM that performs the dynamic calculation and determines the final position as well as velocity of our special type simulator in the virtual scene. Output Component mainly performs publishing the position and rotation of simulator in 3D world.

3 Kinematics analysis of 6-DOF motion platform

Our 6-DOF motion platform is a hydraulic-driving hexapod steward motion platform. With a fixed platform on the ground, a moving platform above and six hydraulic cylinders as the hinge of them, the motion simulator can render the spatial 6-DOF motion. As the same as the hinges fixed between the fulcrums of the top platform and hydraulic piston-rods, spherical hinges are fixed between the fulcrums of the base platform and hydraulic cylinders.

The structure of the platform at the initial position is shown as the Fig. 3. C_p and C_f is respectively the center of the top platform and the base platform. Oppositely, F_i and G_i (i=1, 2, …, 6) is respectively the corresponding fulcrum of the top platform and the base platform.

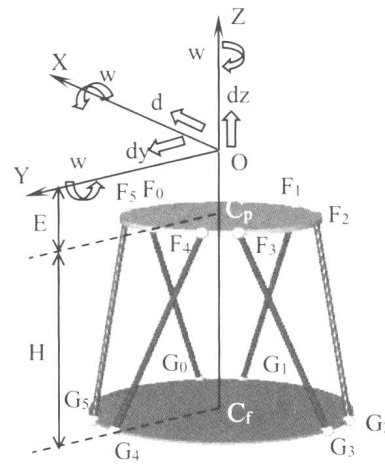

Fig. 3 The structure of the platform I

Suppose that the coordinate of F_i and G_i is $F_i(f_{ix}, f_{iy}, f_{iz})$ and $G_i(g_{ix}, g_{iy}, g_{iz})$ respectively. As the running posture shown in the Fig. 4, suppose the distance of the top platform translated along X-axis, Y-axis and Z-axis is respectively d_x, d_y, d_z, the angle swept around the axes is respectively w_x, w_y, w_z and the new coordinate of the fulcrum F_i is $F_i'(f_{ix}', f_{iy}', f_{iz}')$. Then get the following equation.

$$\begin{bmatrix} f_{ix}' \\ f_{iy}' \\ f_{iz}' \end{bmatrix} = \begin{bmatrix} a_{11} & a_{12} & a_{13} \\ a_{21} & a_{22} & a_{23} \\ a_{31} & a_{32} & a_{33} \end{bmatrix} \cdot \begin{bmatrix} f_{ix} \\ f_{iy} \\ f_{iz} \end{bmatrix} + \begin{bmatrix} d_x \\ d_y \\ d_z \end{bmatrix} \quad (1)$$

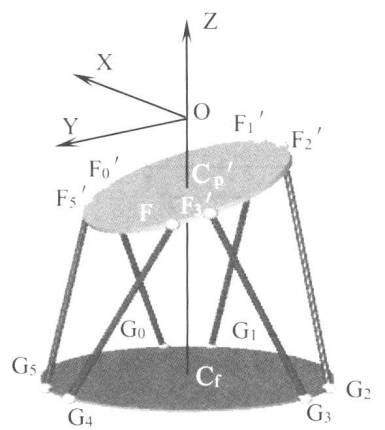

Fig. 4 The structure of the platform II

In the equation (1), a_{11}=cos(w_z)·cos(w_x), a_{21}=-sin(w_z)·cos(w_y), a_{13}=cos(w_z)·sin(w_y)·cos(w_x)+sin(w_z)·sin(w_x), a_{22}= sin(w_z)·sin(w_y)·sin(w_x)+cos(w_z)·cos(w_x),

a_{23}= -sin(w_z)·sin(w_y)·cos(w_x)+cos(w_z)·sin(w_x),
a_{31}= -sin(w_y), a_{32}=-cos(w_y)·sin(w_x), a_{33}=cos(w_y)·cos(w_x).

Also suppose the length of the cylinder (from the hinge at the base platform to the hinge at the top platform) at the initial position is L_i and the one while running is L_i'. Then we can get the equation as follows.

$$L_i = \sqrt{(g_{ix} - f_{ix})^2 + (g_{iy} - f_{iy})^2 + (g_{iz} - f_{iz})^2}$$
$$L_i' = \sqrt{(g_{ix} - f_{ix}')^2 + (g_{iy} - f_{iy}')^2 + (g_{iz} - f_{iz}')^2} \quad (2)$$

So, the result of the inverse displacement analysis of 6-DOF platform can be described as follows.

$$d_i = L_i' - L_i \quad (i=1, 2, \ldots, 6) \quad (3)$$

Finally, we get the control signal of the every cylinder of the 6-DOF platform as follows.

$$ST_i = L_i' - L_i \quad (4)$$

4 Synchronous record of the motion simulator

The implement of synchronous record of the motion simulator comprises with acceleration sensors measuring acceleration motion signal of 6-DOF, A/D translator card and the original interface circuit.

4.1 Principle of recording the 6-DOF motion

Fig. 5 shows the installation of the acceleration sensors and the coordinate system. Three of sensors, A, B, C, are fixed at the vertexes of a regular triangle. AC linked line is parallel to the X-axis and the center of the triangle coincides with the coordinate origin where sensor E is fixed. Sensor F and D is placed respectively on the positive and negative half of X-axis. The distance of line segment DE and EF are equality.

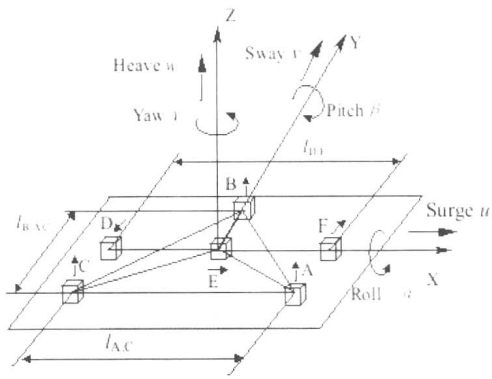

Fig. 5 Method of measuring 6-DOF motion

The measuring direction of each sensor is shown as the arrow pointed in the figure: the directions of sensor A, B are along with the positive half of Z-axis. The directions of sensor F, D are along with the positive and negative half of Y-axis and the direction of sensor E is along with the positive half of X-axis. We set that the acceleration measured by Sensor A is a_A and the same to the other sensors. Then, the accelerations of the triangle center of the translation between front and back, left and right, and up and down can be obtain respectively as follows.

$$a_{Surge} = a_F, \quad a_{Sway} = \frac{a_F - a_D}{2}, \quad a_{Heave} = \frac{a_A + a_B + a_C}{3} \quad (5)$$

The acceleration of flip, pitch and rotation respectively is:

$$\varepsilon_{Roll} = \frac{a_B - (a_A + a_C)/2}{l_{B\text{-}AC}}, \quad \varepsilon_{Pitch} = \frac{a_C - a_A}{l_{A\text{-}C}}, \quad \varepsilon_{Yaw} = \frac{a_F + a_D}{l_{D\text{-}F}} \quad (6)$$

According to the above formulas, the accelerations of the triangle center can be calculated, including three translation accelerations and three angular accelerations. With low-pass filter and twice digital integration, we can obtain linear displacement u, v, w and angular displacement α, β, γ. With the Inverse displacement analysis of 6-DOF platform, we can calculate the extension of six hydraulic cylinders. By the method of PID control, a spatial 6-DOF motion can be performed by the simulation system.

4.2 Analysis of the motion track

With the method of synchronous record, the running track of hydraulic cylinders can be obtained. Then, we compare the running track, shown in Fig. 6 with the full line, with the track collected from a real vehicle, shown with the dotted line.

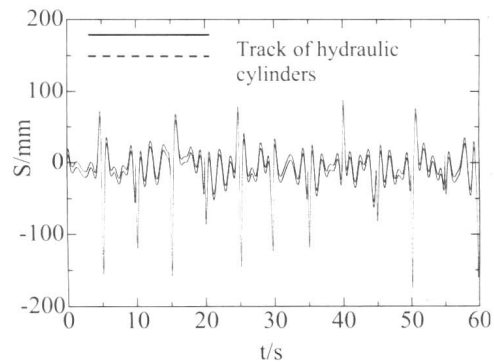

(a) Track recorded in 10 min

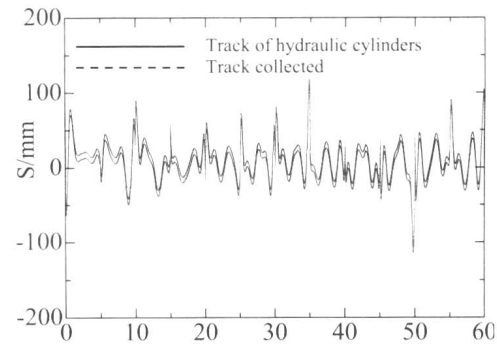

(b) Track recorded in 20min

Fig. 6 Real vehicle tracks collected and hydraulic cylinder tracks recorded

As the figure showing, there is almost no different between them. During the experiments, the data of motion recorded respectively in 10min, 20min and 30min. All of the experiments achieved satisfactory results. According to the results, our motion simulation system runs smoothly and the software is reliably. So, the design requirements can be met.

5 Conclusions

With a 6-DOF motion, a 180 degree forward field-of-view and spatial sound, our motion simulation system can provide a high immersion feeling of Virtual Reality. Comparing the hydraulic cylinder tracks recorded by the method of synchronous record with the real vehicle tracks collected from a real vehicle, the system has been proved to be smoothly and reliably, which could be really meaningful for farther research in the vehicle system, human factor study and training of driving skills.

Acknowledgments

The work is supported by the Industrialization and Generalization of Motion Simulation On-line and Synchronous-Recording Technique (No. 20085006) and the Fund from the Jilin University Basic Scientific Research Bursary (No. 200903167).

References

[1] Tao Ni, DingXuan Zhao, Hongyan Zhang. Realistic vehicle driving simulator with dynamic terrain deformation[C], Proceeding of the 2009 IEEE International Conference on Mechatronics and Automation, Aug. 9-13. Chuangchun, China, 2009: 4795-4800.

[2] Mingde Gong, Bo Tian. Design 6-DOF fatigue life test system for vehicle driver seat[C], Mechanic Automation and Control Engineering (MACE), 2011 Second International Conference, Jul. 15-17, Hohhot, China, 2011: 1140-1143.

[3] Tao Ni, Yamada H., Zhang H.. Image based real-time 3D reconstruction for teleoperation system[C], IEEE International Conference on Computer, Mechatronics, Control and Electronic Engineering (IEEE CMCE), Jul., 2010: 265-268.

[4] Ni T., Zhao D., Ni S., Zeng C.. Graphical simulation of remote control construction robot based on Virtual Reality[C], Transactions of the Chinese Society for Agricultural Machinery, vol. 36, 2005: 80-82.

[5] Zhao D., Yamada H., Mukaida S.. Study on method to prepare sence of presence with 3 degree of freedom oscillation apparatus[C], Proceeding Annual Meeting, Japan Society of Mechanical Engineers, 1999,4: 13-16.

Research on the Closed Hydraulic Regeneration System of the Boom Potential Energy in Hybrid Excavators

Zhao Dingxuan *, Zhang Zhengfei, Hao Tianqi

College of Mechanical Science and Engineering, Jilin University, Changchun 130022, China
* Corresponding Author: zdx@jlu.edu.cn

Abstract Aimed at the hybrid excavators, an energy recovery scheme with hydraulic accumulator for boom cylinder is put forward. The simulation model of hybrid hydraulic excavator with the regeneration system is built, and the energy recovery effects of the closed system for boom are calculated. The test-bed of hybrid excavator for energy regeneration with hydraulic accumulator is constructed, in virtue of the test-bed, investigated about the energy recovery effects of the regeneration system. The results of simulation and experiment show that the closed hydraulic regeneration system of the boom potential energy in hybrid excavators is feasible, which has a high recovery efficiency.

Keywords Hydraulic excavators; Hybrid; Closed regeneration system; Hydraulic accumulator; Simulation in Simulink.

1 Introduction

Hydraulic excavator is the one of the most widely used engineering machinery, because of its efficiency, durable and strong adaptability, and plays a pivotal role in economic construction. But at the same time, hydraulic excavator is also a kind of high fuel consumption, poor emission and serious environmental pollution engineering machinery. As the number of hydraulic excavator is more and more, its energy conservation and environmental protection issues are becoming increasingly urgent and serious. As hybrid energy saving and energy recycling technology have been successfully applied in automobile industry, people show a keen interest in its application in engineering machinery.

In excavators work process, the boom is up and down frequently. With the boom is falling down, the hydraulic fluid in the boom cylinder of traditional excavators flow to tank directly without energy regeneration. Because of the large inertia of the boom, when the boom is falling down, a large amount of energy will be released, which is not only wasteful but also leading to heating the system. In order to reduce the energy consumption and the heat, energy recovery is a more effective measure. And the hybrid hydraulic excavator with energy recovery system can store up the gravitational potential energy of the boom. However, traditional energy recovery system is not suitable for energy recovery hydraulic excavator.

The following are two typical types of energy recovery system for excavators.

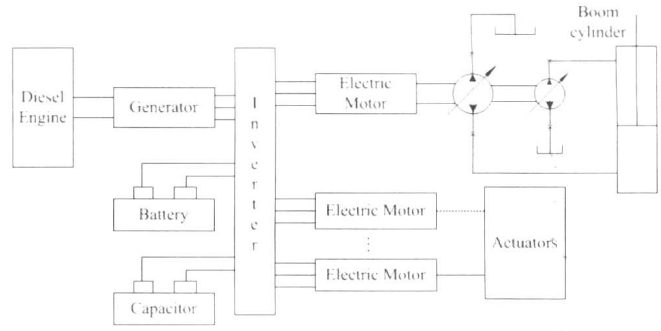

Fig. 1 Recovery system of hybrid excavator

The scheme proposed in Ref. [1] is shown in Fig. 1. The regeneration system and the control strategy of the scheme are simple, however, it will lead to additional energy consumption and reduce electric motor life, due to frequent reversing of motor, and the recovery effects is not obvious.

The scheme proposed in Ref. [2] is shown in Fig. 2. The system used a hydraulic motor in turn oil loop to avoid the lack of the system shown in Fig. 1, showed some effects of regeneration[2]. However, the above systems are required to convert the mechanical energy into hydraulic energy, and then convert into electrical energy to be stored, and when it is needed, the energy is converted back oppositely. Too many energy conversion links and the low conversion efficiency of each link lead to a poor effect of recovery.

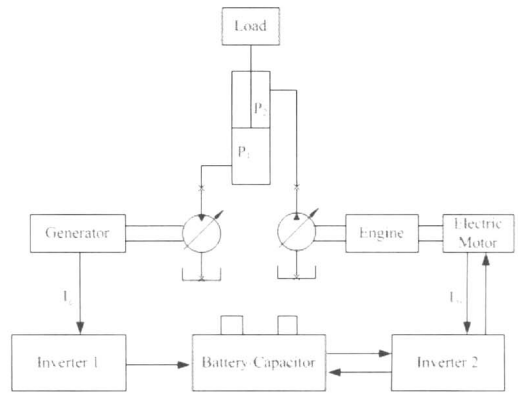

Fig. 2 Recovery system with hydraulic motor

In addition, by storing up the regenerated energy in the hydraulic accumulator, the regeneration system avoided too

many conversion links and improved the recovery efficiency, which attracts more attention of the experts.

This paper firstly presents a closed hydraulic regeneration system based on hydraulic accumulator, and then carries out the simulation and experimental studies. The results of simulation and experiment show that the closed hydraulic regeneration system of the boom potential energy in hybrid excavators is feasible, which has a high recovery efficiency.

2 The structure of the closed regeneration system

Fig.3 is the diagram of the closed recovery system based on hydraulic accumulator. As shown in Fig. 3, two bidirectional quantitative pump/motors are used, one of the ports of the pumps is connected respectively with the rod chamber of the boom cylinder(9) and accumulator(8), and another one is connected with the rodless chamber, bidirectional quantitative pump/motors were driven by electric motor. The flow ratio of the two bidirectional quantitative pump/motors is 1:(K-1), where K is area ratio of the rod chamber and rodless chamber, which can ensure the oil flow of rod chamber and rodless chamber keep balance. Three groups of relief valve and check valve protect the system from being damaged.

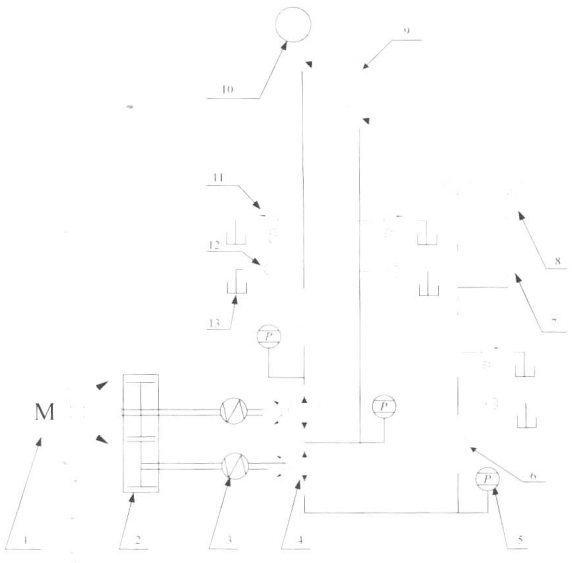

Fig. 3 The closed hydraulic regeneration system
1—Motor; 2—Transfer case; 3—Torque-Speed transducer;
4—Quantitative pump / motor; 5—Pressure transducer;
6—Flow meter; 7—Stop valve; 8—Accumulator;
9—Boom cylinder; 10—Load; 11—Relief valve;
12—Check valve; 13—Tank

As the boom is falling down, one part oil of rodless chamber flow back to rod chamber, and another one flow to accumulator through the pumps. When the system upholds objects, the energy stored in accumulator is released, which can promote the two pumps together with the electric motor. In the initial phase of the experiment, oil need to be injected into the hydraulic system and the system need to fill or unload oil, therefore, relief valve is designed for unloading oil and the check valve is designed to fill the system with oil.

3 Simulation research on the closed regeneration system

In order to verify the feasibility of the regeneration system, a system model is established, and simulation study with the Matlab/Simulink is carried out. The simulation research for one accumulator or two accumulators at different inflation pressures were studied. The results are shown in Figs. 4 and 5.

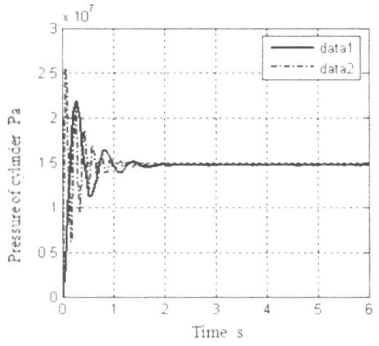

(a) Pressure curves of hydraulic cylinder

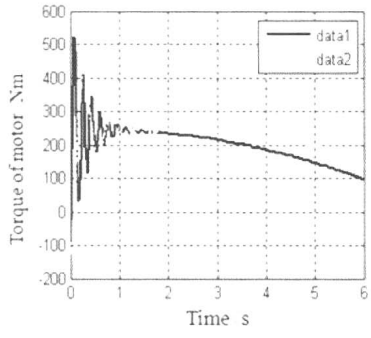

(b) Output torque of motor

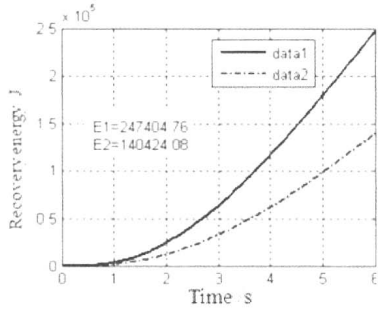

(c) Accumulator energy recovery curves

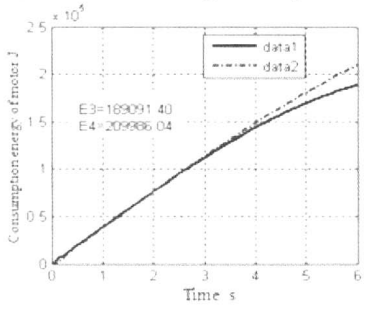

(d) Motor energy curves

Fig. 4 Simulation curves when the inflation pressure of accumulator is at 10MPa